Linear and nonlinear waves on coating entrance menisci

R. G. Keanini*, Justin A. Thompson, and Kiran Gona

Department of Mechanical Engineering and Engineering Science

The University of North Carolina at Charlotte

Charlotte, North Carolina 28223-0001

Abstract

The response of optical fiber ribbon entrance menisci to impulsive lateral motion of the ribbon or coating die is theoretically investigated. In the limit where the characteristic axial coating pressure increase along the meniscus is much larger than the characteristic gas viscous shear stress along the meniscus, the meniscus free surface is described by a nonlinear wave equation. Here, surface discontinuities, analogous to shocks, appear when the spacing between the fiber and die decreases; shock propagation into the moving fiber in turn is proposed as a potentially important bubble forming mechanism. By contrast, when spacing between the fiber and die increases, expansion fans form in the characteristic x-t plane, leading to gradual, rather than abrupt changes in the meniscus shape. Linear waves are predicted for a range of conditions; in this case, any time-varying

*Corresponding Author. Address: Mechanical Engineering & Engineering Science, UNC-Charlotte, 9201 University City Blvd, Charlotte, NC 28223-0001. Email: rkeanini@uncc.edu; Phone: 704-687-8336; Fax: 704-687-8345

change in the distance between the die entrance and fiber ribbon propagates at fixed speed, without distortion, down the meniscus.

Mathematics Subject Classification: 76D33

Keywords: fiber coating; free surface waves

Introduction

The formation of bubbles in fiber optic coatings remains a significant, poorly understood problem. In particular, trapped coating bubbles can produce microbends within the fiber, which in turn can lead to significant signal attenuation [1–3]. Process features associated with bubble formation in fiber coatings include process gas entrainment by the fiber as it passes through the coating reservoir [4–7] and bubble nucleation of dissolved gases during, and subsequent to, the coating operation [3].

A typical high speed fiber ribbon coating process, depicted schematically in Fig. 1, passes a ribbonized set of fibers through a coating die, at speeds on the order of 10-30 m/s. An entrance meniscus, which can exhibit a range of width to depth ratios, forms where the ribbon plunges into the liquid coating. Although a number of experimental investigations have studied gas entrainment via breakdown of the entrance meniscus [4–8], due to the complexity of in-die process physics, characterized by coupled, fiber-driven gas and liquid flows, a gas-liquid interface, material-, speed-, temperature-, and surface-roughness-dependent dynamic contact lines, and rapid gas dissolution into the liquid phase [9], relatively few theoretical studies of in-die fluid mechanics have been undertaken; see, e.g., the brief review in [1] as well as references in [10, 11]. With regard to the

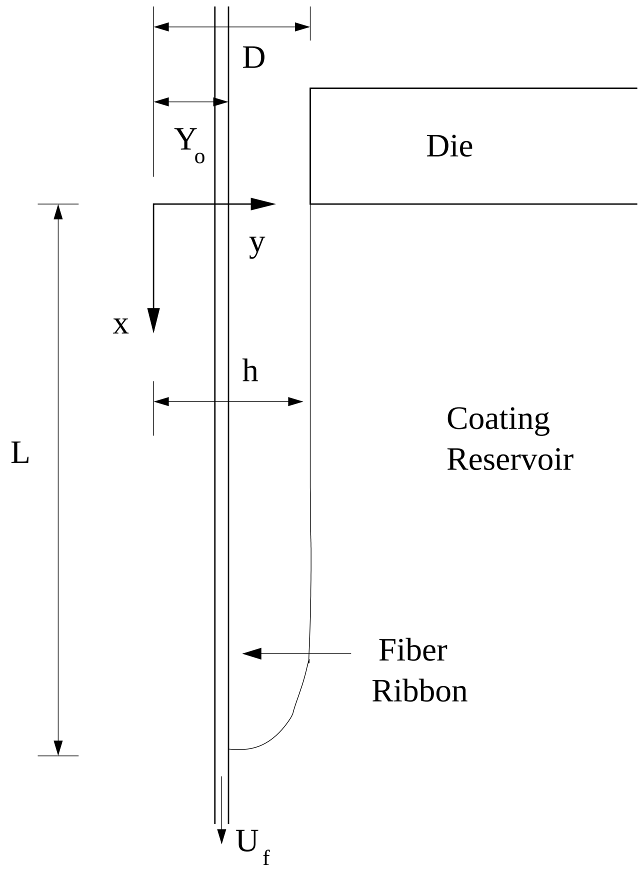

Figure 1: Schematic of entrance meniscus region of a fiber ribbon coating operation.

dynamics of the entrance meniscus, very little theoretical work has likewise been reported [12].

This short note considers the response of the entrance meniscus to impulsive lateral motion of either the coating die or fiber ribbon. It is found that when the characteristic coating pressure increase along the meniscus is much larger than the characteristic gas shear stress along the meniscus, the meniscus is governed by a nonlinear wave equation. In this case, impulsive lateral die motions which reduce the distance between the die and fiber ribbon produce shock wave-like disturbances on the entrance meniscus; impulsive die motions that increase this distance, by contrast, lead to expansion fan-like free surface disturbances. Linear wave behavior occurs under a wide range of conditions; here, any time-varying change in the distance between the die entrance and fiber ribbon propagates at fixed speed, without distortion, down the meniscus. We suggest that propagation of nonlinear and linear free-surface shocks into the moving fiber represents an important bubble-forming mechanism.

Entrance meniscus model description

A detailed derivation of the entrance meniscus model can be found in [3]; here, we present model assumptions and the main results. Again, a schematic of the ribbon-coating process is shown in Fig. 1. Typical length scales are as follows [3]: the fiber ribbon thickness is on the order of 250 μm, the meniscus length, $\tilde{L}$, is on the order of 1 mm (for fiber travel speeds on the order of 10-30 m/s), and the nominal clearance, $\tilde{D}$, between the ribbon face and die entrance, corresponding to the maximum thickness of the gas-filled gap between the ribbon and meniscus, is 17.5 μm. A ribbon consisting of 12 fibers is approximately 3 mm wide. [Note, in the following, dimensional quantities are denoted with tildas; all other terms are nondimensional.]

Key model assumptions are as follows. First, based on both the limited axial extent of the meniscus, again on the order of 1 mm, and based on computed pressure distributions within a typical coating die applicator [1] (indicating an approximate linear increase in pressure along the entry meniscus), we assume that the liquid-side pressure increases linearly with the coordinate $\tilde{x}$. This assumption, introduced in order to circumvent calculation of the coating flow field, is designed to capture the large pressure gradients extant within pressurized coating applicators. Thus, the near-meniscus liquid-side pressure gradient is treated as a parameter. Second, we assume that the coating liquid behaves as a Newtonian fluid [10]. Third, dissolution of process gas into the coating liquid [9] is not accounted for. Finally, based on experimental observations [3], it is assumed throughout that the aspect ratio, $\epsilon = \tilde{D}/\tilde{L}$, of the gas-filled gap between the moving fiber and meniscus is small, $\epsilon << 1$.

The equation governing the meniscus free surface is obtained as follows. First, due to the narrowness of the gas-filled gap, the leading order gas velocity field is shown in [3] to be governed by equations corresponding to the lubrication approximation. Second, due to negligible transverse gas velocities, normal viscous stresses on each side of the free surface are likewise negligible so that the normal stress balance simplifies to the Young-Laplace equation. Third, imposition of the kinematic condition at the free surface, integration of the gas-phase continuity equation across the gap, and allowance for purely lateral motion of the fiber ribbon [i.e., $\tilde{Y}_o = \tilde{Y}_o(\tilde{t})$], then leads to the following leading order nondimensional equation governing the free surface shape, $h = h(x, t)$:

$$h_{o,t} + H_1 h_{o,xxxx} + H_2 h_{o,xxx} + H_3 h_{o,x} - \dot{Y}_o = 0 \tag{1}$$

where

$$H_1 = \frac{A_2}{2}\left[\frac{h_o^3}{6} - \frac{Y_o^3}{6} + \frac{h_o Y_o^2}{2} - \frac{h_o^2 Y_o}{2}\right]$$

$$H_2 = \frac{A_2}{4}\left(h_o - Y_o\right)^2 h_{o,x}$$

and

$$H_3 = -\frac{A_1}{4}\left(h_o - Y_o\right)^2 + \frac{1}{2}$$

Here, the dimensionless gas velocity and meniscus shape, represented collectively as χ, have been expanded as $\chi = \chi_o + \epsilon_1\chi_1 + \epsilon^2\chi_2 + \ldots$, where $\epsilon_1 = \epsilon Re = \epsilon(\tilde{U}_f\tilde{D}/\tilde{\nu}_g)$, $Re = O(1)$ is the characteristic Reynolds number for the gas flow within the gap, $\tilde{U}_f$ is the characteristic fiber speed, and $\tilde{\nu}_g$ is the gas kinematic viscosity. Thus, h_o is the leading order term in the expansion for h. Again, as shown in Fig. 1, Y_o is the instantaneous horizontal displacement of the fiber from its neutral position.

The parameters A_1 and A_2 are defined as $A_1 = \epsilon(\tilde{G}\tilde{L})(\tilde{\mu}_g\tilde{U}_f/\tilde{D})^{-1}$ and $A_2 = \epsilon^3(\tilde{\gamma}/\tilde{D})(\tilde{\mu}_g\tilde{U}_f/\tilde{D})^{-1}$, where $\tilde{\mu}_g$ is the gas viscosity, $\tilde{G}$ is the coating axial pressure gradient, and $\tilde{\gamma}$ is the coating surface tension coefficient. Physically, A_1 represents the ratio of the characteristic change in coating pressure over the length of the meniscus, $\tilde{P}_l = \tilde{G}\tilde{L}$, to the characteristic shear stress, $\tilde{\tau}_g = \tilde{\mu}_g\tilde{U}_f/\tilde{D}$, exerted by the gas on the reservoir, scaled by the aspect ratio, ϵ. Likewise, A_2 represents the ratio of the characteristic capillary pressure due to coating surface curvature, $\tilde{\sigma}_{ST} = \tilde{\gamma}/\tilde{D}$, to the characteristic gas shear stress, $\tilde{\tau}_g$, scaled by ϵ^3. Finally, note that nondimenionalization is carried out using the following respective velocity, pressure, time, axial-length, and lateral-length scales: $\tilde{U}_f$, $\tilde{\rho}_a\tilde{U}_f^2$, $\tilde{L}/\tilde{U}_f$, $\tilde{L}$, and $\tilde{D}$.

Results and discussion

In the following, we consider free surface response to impulsive movement of the coating die or fiber ribbon, focusing on several limiting cases. In the cases considered, the undisturbed, steady state entrance meniscus is found [3] to have a constant width, $h_o(x) = 1$, equal to the distance, $D = 1$, between the die entry and the ribbon; as discussed in [3], the steady solution breaks down in the vicinity of the dynamic contact line.

Linear free surface waves

We consider first the linear response of the meniscus under conditions where $A_1 << 1$ and $A_2 << 1$. Due to the ϵ scaling of the ratio of the characteristic axial coating pressure change, $\Delta\tilde{P}_l$, to gas shear stress, $\tilde{\tau}_g$, in A_1, and due to the ϵ^3 scaling of the ratio of capillary pressure, $\tilde{\sigma}_{ST}$, to $\tilde{\tau}_g$ in A_2, the present limits apply to a broad range of conditions: $0 < \Delta\tilde{P}_l/\tilde{\tau}_g << \epsilon^{-1}$ and $0 < \tilde{\sigma}_{ST}/\tilde{\tau}_g << \epsilon^{-3}$. Referring to (1) and using the substitution $u(x,t) = h_o(x,t) - Y_o$, where $u(x,t)$ represents the instantaneous local gap thickness between the meniscus and fiber, we arrive at a simple linear first order wave equation in u :

$$u_{,t} + \frac{1}{2}u_{,x} = 0 \tag{2}$$

In this limit, information concerning changes in either the die entrance width, $\tilde{D}$, or fiber ribbon position, $\tilde{Y}_o$, thus travels at half the speed of the fiber (where the nondimensional fiber speed is 1).

Considering, for example, the case where the entrance gap, $\tilde{D}$, instantaneously increases or decreases, we arrive at a signaling problem [13] and can use a characteristic diagram to determine the meniscus response. Refer to Fig. 2. Here, possible reflections at the dynamic contact line are neglected as well as capillary and viscous smoothing of the surface discontinuities created. Due to the linearity of the problem, and in contrast to the nonlinear case discussed below, any given discontinuity propagates at speed 1/2. Thus, any time-dependent change in the die entrance width, $\tilde{D}$, propagates down the meniscus without distortion or dispersion. From a practical standpoint, this result is important since it suggests that wave propagation into the moving fiber represents a potential coating bubble formation mechanism.

A similar approach can be used to examine meniscus response to lateral shifts in fiber position,

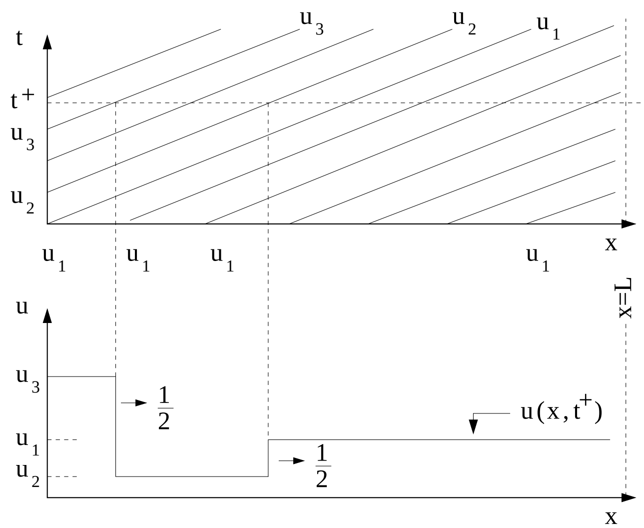

Figure 2: Meniscus response to time varying die motion - linear regime.

Y_o. In this case, it is readily shown that an outward movement of the fiber ribbon (away from the die entrance) leads to a linear-in-time increase in the length, L, of the gas pocket. While the model predicts that an inward displacement also produces a similar increase in L, consideration of the free surface normal stress balance in the vicinity of the dynamic contact line, $\tilde{P}_g - \tilde{P}_l \approx \tilde{\gamma}/\tilde{r}$, where $\tilde{r}$ is the characteristic surface curvature, shows that the only physically realizable possibility is the first. In particular, since $\tilde{P}_g \approx \tilde{\rho}_g \tilde{U}_f^2$ is essentially fixed while $\tilde{P}_l$ increases with depth $\tilde{x}$, then since outward ribbon movements lead to increased $\tilde{r}$, the dynamic contact line must move downward to a location where the difference in gas dynamic pressure and coating pressure satisfies the stress balance.

Nonlinear waves - shocks and expansion fans

We shift now to the nonlinear response of the meniscus under conditions where $A_1 = O(1)$ and $A_2 << 1$. Here, the characteristic gas shear stress within the gap, $\tilde{\tau}_g$, is much smaller than the characteristic axial change in coating pressure, $\Delta\tilde{P}_l$ $[\tilde{\tau}_g/\Delta\tilde{P}_l = O(\epsilon)]$. By contrast, and as in the linear case, the constraint $A_2 << 1$ is not particularly limiting. Under these conditions, (1) simplifies to the following nonlinear wave equation in $u(x,t) = h_o(x,t) - Y_o$:

$$u_{,t} + \frac{1}{2}(1 - \frac{1}{2}A_1 u^2)u_{,x} = 0 \tag{3}$$

Due to nonlinearity, a rich set of surface responses are now possible; we illustrate with two examples. For simplicity, we limit attention to $A_1 D^2/2 < 1$, where $D = \tilde{h}_o(\tilde{x} = 0, \tilde{t})/\tilde{D}$ and $u \le D$ for all x and t. In this case, and for increasing time t, characteristics are directed in the positive $x-$ direction. [When $A_1 u^2/2 > 1$, characteristics are directed in the negative $x-$ direction (with increasing t), and run parallel to the $t-$ axis when $A_1 u^2/2 = 1$. Left-running characteristics undergo reflection at the die entrance; a detailed method of characteristics construction can be undertaken in this case.] In the first example, the fiber ribbon remains fixed laterally, while the die entrance width, $\tilde{D}$, instantaneously decreases from $D_1 = 1$ to D_2. Since wave speed, $c = (1/2)[1 - A_1 u^2/2]$, increases with decreasing gap width, u (and vice-versa), then as shown in Fig. 3, a free surface discontinuity forms immediately. In the following discussion, we will refer to these discontinuities as *shocks*. Using a standard shock fitting procedure [13], we find that the shock speed, c_s, is given by

$$c_s = \frac{1}{2} - \frac{A_1}{2}[u_2^2 + u_1 u_2 + u_1^2] \tag{4}$$

where u_1 and u_2 are, respectively, the gap thicknesses before and after die displacement; refer to Fig. 3. Again, we are neglecting capillary and viscous smoothing and possible reflection at the

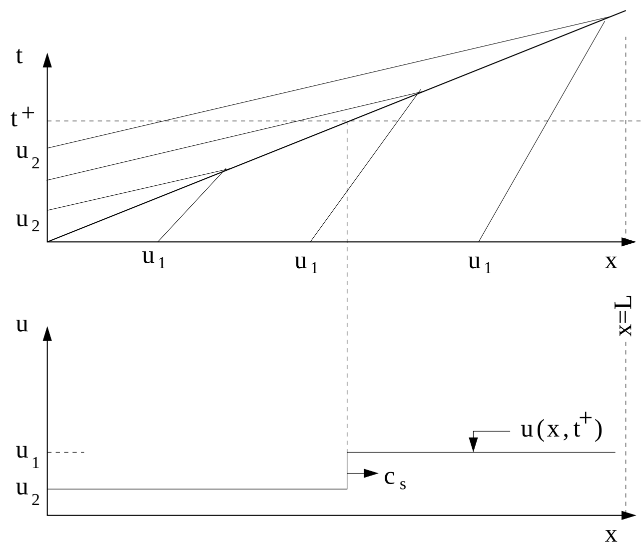

Figure 3: Meniscus response to impulsive inward die motion - nonlinear regime.

nominal dynamic contact line. Again, analogous to the linear response case, shock propagation into the moving fiber may represent an important coating bubble formation mechanism.

Another practically important circumstance concerns meniscus response to *small* inward shifts in die position. Thus, letting $u_2 = u_1 - \epsilon_o$, where $\epsilon_o << u_1$, it is readily shown that wave speeds before and after the *weak* shock, given respectively by $c_1 = 1/2 - A_1 u_1^2/4$, and $c_2 = c_1 + A_1 u_1 \epsilon_o/2 + O(\epsilon_o^2)$ satisfy $c_1 > c_s > c_2$, where $c_s = c_1 + A_1 u_1 \epsilon_o/4 + O(\epsilon_o^2)$, and where $u_1 = 1$ for $Y_o = 0$. Thus, in this case, the shock speed differs only slightly from the wave speed associated with the undisturbed meniscus, c_1. [Note, wave speeds ahead of and behind any shock always satisfy the above set of inequalities.]

As a second example, we consider the nonlinear response when the fiber ribbon again remains laterally fixed while the die entrance width *increases* instantaneously from $D_1 = 1$ to D_2. As shown in Fig. 4, in this case, an expansion fan forms in the characteristic $x - t$ plane, and again allows

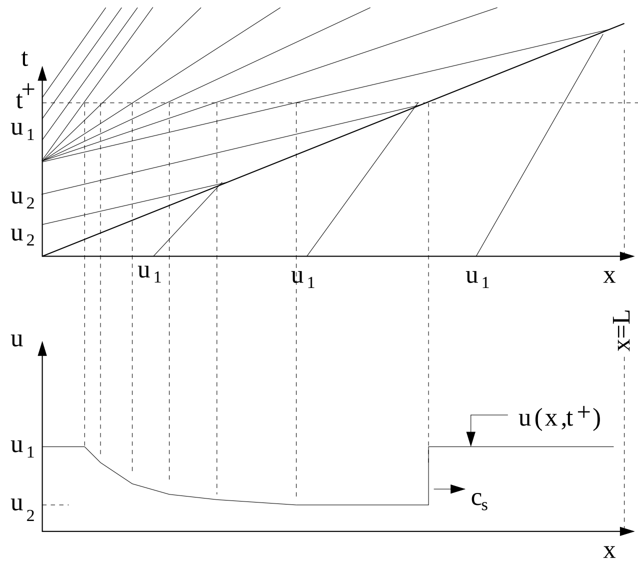

Figure 4: Meniscus response to impulsive inward die motion followed by impulsive outward motion (to original position) - nonlinear regime.

ready construction of the time-varying meniscus shape. [Note, Fig. 4 shows an example where an initial decrease in entry width is followed by an increase.] Concerning potential bubble formation during impingement of an expansion fan on the dynamic contact line, it does not appear that this represents a plausible mechanism. Since expansion fan impingement both reduces free surface curvature (in the vicinity of the dynamic contact line) and forces the contact line downward to regions of higher coating liquid pressure, there is no apparent mechanism, for example, to cause the contact line to rebound against the incoming expansion fan. Clearly, however, detailed examination of the near-contact-line region is required in order to address questions of this kind.

References

[1] S-Y. Yoo and Y. Jaluria, Isothermal flow in an optical coating applicator and die system, J. Lightw. Tech. 24 (2006), 449-463.

[2] S. Torza, The continuous coating of glass fibers, J. Appl. Phys. 47 (1976), 4017-4020.

[3] J. A. Thompson, Physical investigation and analytical modeling of coating process used in optical fiber ribbon manufacturing, Ph.D. dissertation, Univ. North Carolina at Charlotte, 2005.

[4] R. Burley and J.P.S. Jolly, Entrainment of air into liquids by a high speed continuous solid surface, Chem. Eng. Sci. 39 (1984), 1357-1372.

[5] U.C. Paek, High-speed high-strength fiber drawing, J. Lightw. Tech. LT-4 (1986), 1048-1060.

[6] A. Abraham and C. Polymeropoulos, Dynamic menisci on moving fibers, Proc. 48th Int. Wire Cable Symp., pp. 520-524, Atlantic City, NJ, 1999.

[7] S. Ravinutala and C. Polymeropoulos, Entrance meniscus in a pressurized optical fiber coating applicator, Exp. Therm. Fluid Sci. 26 (2002), 573-580.

[8] S. Ravinutala, K. Rattan, C. Polymeropoulos and Y. Jaluria, Dynamic menisci in a pressurized fiber applicator, Proc. 49th Int. Wire Cable Symp., pp. 474-478, Atlantic City, NJ, 2000.

[9] D. Jacqmin, Very, very fast wetting, J. Fluid Mech. 455 (2002), 347-358.

[10] D. Quere, Fluid coating on a fiber, Annu. Rev. Fluid. Mech. 31 (1999), 347-384.

[11] S.J. Weinstein and K.J. Ruschak, Coating Flows, Annu. Rev. Fluid Mech. 36 (2004), 29-53.

[12] A.S. Biriukov, V.A. Bogatyrjov and A.G. Khitun, On the origin of periodic inclusions in metals frozen onto a moving substrate, J. Appl. Phys. 81 (1997), 7018-7023.

[13] G.B. Whitham, Linear and Nonlinear Waves, Wiley, New York, 1974.